

I Don't Need \mathbf{u} : Identifiable Non-Linear ICA Without Side Information

Matthew Willetts

University College London & The Alan Turing Institute

MWILLETTS@TURING.AC.UK

Brooks Paige

University College London & The Alan Turing Institute

BPAIGE@TURING.AC.UK

Abstract

In this work we introduce a new approach for identifiable non-linear ICA models. Recently there has been a renaissance in identifiability results in deep generative models, not least for non-linear ICA. These prior works, however, have assumed access to a sufficiently-informative auxiliary set of observations, denoted \mathbf{u} . We show here how identifiability can be obtained in the absence of this side-information, rendering possible fully-unsupervised identifiable non-linear ICA. While previous theoretical results have established the impossibility of identifiable non-linear ICA in the presence of infinitely-flexible universal function approximators, here we rely on the intrinsically-finite modelling capacity of any particular chosen parameterisation of a deep generative model. In particular, we focus on generative models which perform clustering in their latent space — a model structure which matches previous identifiable models, but with the learnt clustering providing a synthetic form of auxiliary information. We evaluate our proposals using VAEs, on synthetic and image datasets, and find that the learned clusterings function effectively: deep generative models with latent clusterings are empirically identifiable, to the same degree as models which rely on side information.

1. Introduction

When evaluating the performance of a deep generative model (DGM) with latent variables, there are two primary concerns. The first is the quality of the fit to the data: i.e., to what extent does the learned model approximate the distribution of the underlying data. This includes checking whether synthetic generations from the trained model look like plausible “real” data. Evaluating the fit of the model to the data typically involves integrating out the latent variables.

The second slightly-more-elusive concern is whether we can ascribe any particular meaning or utility to the latent variables themselves. Linear methods such as probabilistic principal components analysis (Tipping & Bishop, 1999), and nonlinear methods such as variational autoencoders (Rezende et al., 2014; Kingma & Welling, 2014), associate each data point with a posterior distribution over a low-dimensional latent variable. These posteriors (or summaries, such as the posterior mean) are often hoped to be useful for downstream tasks, as unsupervised representations; they also are often hoped to correspond to underlying ground-truth or statistically independent factors of variation. Much recent work has focused on the question of learning variational autoencoders with “disentangled” representations (Higgins et al., 2017; Kim & Mnih, 2018; Chen et al., 2018; Esmaeili et al., 2019), with mixed results (Locatello et al., 2019; Rolinek et al., 2019).

One particular useful criteria is the *identifiability* of the latent representations of the model. At its core, identifiability captures a notion of whether the model can be accurately and consistently learned, given data. In the deep generative model setting, we are particularly interested in the identifiability of the latent variables. In highly flexible models, multiple settings of parameters could define the

same probability distribution (i.e., the parameters are not identifiable), while still having a latent representation which is the same across these different parameters (Hyvärinen & Morioka, 2016; Hyvarinen et al., 2019; Khemakhem et al., 2020a; Li et al., 2020; Sorrenson et al., 2020; Khemakhem et al., 2020b; Roeder et al., 2021). A standard definition of identifiability of latent representations used in deep generative models is that different models’ learnt representations are only an affine transform away from each other (Hyvärinen & Morioka, 2016; Khemakhem et al., 2020a; Roeder et al., 2021). It is often this form of identifiability that a) is tested empirically when discussing the identifiability of a given model, including in experiments within primarily theoretical treatments, and b) is of importance to practitioners.

In the last few years there has been a resurgence in identifiability results in machine learning models within certain problem-settings (Hyvärinen & Morioka, 2016; Hyvarinen et al., 2019; Khemakhem et al., 2020a; Li et al., 2020; Sorrenson et al., 2020; Khemakhem et al., 2020b; Roeder et al., 2021). Many of these recent results have been in the space of non-linear ICA, where data has been made by a non-linear mixing of statistically-independent latent sources. Classically the aim is to ‘unmix’ the data, recovering the true sources in the process. For two decades now it has been understood that, for anything other than a lucky subset of problems, it is not theoretically possible to learn a definitive non-linear unmixing when the model being applied by the analyst is a universal function approximator (Hyvärinen & Pajunen, 1999). These recent results provide theory and methods for finding identifiable non-linear unmixing, but all rely on auxiliary side information to sufficiently structure the model’s representations. Informally, the side information is used to ‘break the symmetry’ in the space of representations the model could learn, resulting in a stable and repeatable training procedure. What form of representation you learn depends on what side-information you use – different side-information gives different ‘symmetry-breaking’.

We underline here that these previous theoretical results have been predicated on the idea that our models are infinitely powerful and flexible. In this paper we work within the strand of research into non-linear ICA that aims to learn an appropriate deep generative model for the data. With that approaches one can learn a DGM where the prior in the latent space is conditioned on the given auxiliary information – for VAEs these are known as Identifiable-VAEs (iVAEs) (Khemakhem et al., 2020a). Auxiliary information is necessary to break the symmetries of such a model – when we consider the generative model to be implemented by a universal function approximator – to render it identifiable.

In reality, however, all our models are always of limited capacity. In this work we use the limited capacity of our parametric models to induce a natural auxiliary task to emerge within the model. This task is clustering in the learnt latent space of a deep generative model. The learnt cluster index is then our auxiliary information. Note that iVAEs are also models that implicitly cluster in the latent space, just using the given auxiliary information to identify the appropriate cluster component in the latent space for each data point. We use a particular variety of VAEs with a mixture model in the latent space, VaDE (Jiang et al., 2017), which is in effect an iVAE where the clustering is learnt rather than given. We train these models over a range of different datasets with a range of different neural parameterisations. In each case the parametric form of our deep generative models is sufficiently-determining that, without giving any side-information, the same representations (up to an invertible linear transformation) are learnt each time we train each model architecture on each dataset. We demonstrate our results using encoders and decoders implemented using MLPs, ConvNets and ResNets. We find that our approach, of allowing the model to induce its own natural representations, consistently leads to reproducible representations. By standard empirical measures of the identifiability of the representation, we find performance which matches, or surpasses, provably-identifiable baselines, even without side-information present.

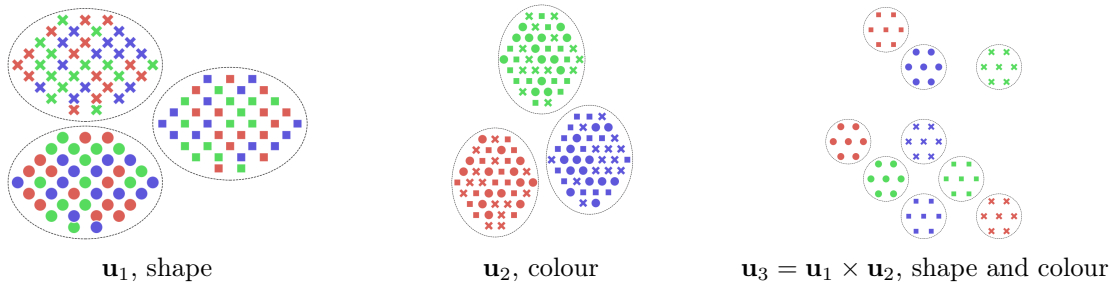


Figure 1: *Different ways to partition a set of objects.* Methods proposed so far that produce identifiable representations rely on being given a particular way, \mathbf{u} , to partition the data being trained on, say \mathbf{u}_1 , the shape of an object. For our purposes as long as our clustering model always learns the same \mathbf{u} -clustering, in this illustrative example it could be shape, colour or both together, we will then obtain identifiable representations.

2. Background

There have been two main paradigms in identifiability results in non-linear ICA. The first is concerned with learning a discriminative model, a classifier, under an appropriate classification task for the data. An example of a task would be identifying what large-scale segment of a temporal sequence a particular observation \mathbf{x} is from (Hyvärinen & Morioka, 2016), or simply predicting the datapoint’s class-label (Hyvarinen et al., 2019).

The dependent variable in our classification task is denoted \mathbf{u} . Using the density ratio trick (Hastie et al., 2017, §14.2.4), one can build a noise contrastive estimation (NCE) loss (Gutmann & Hyvärinen, 2012). The classifier’s predictive probability can be linked to related probabilities in a matching generative model.

If the model is well-trained, the final feature layer of the classifier corresponds to the underlying generating sources, assuming that the chosen and measured \mathbf{u} variable connects to the true generative process for the data. Thus it can then be shown that two classifiers that give the same predictive probabilities produce identifiable unmixed representations (Hyvärinen & Morioka, 2016; Hyvarinen et al., 2019). This setting induces identifiability, up to the choice of classification task; different tasks will lead to different learnt representations.

The second, more recent, strand is based around learning a generative model that embodies both the non-linear procedure that generated the data and a (perhaps approximate) method of inverting it (Khemakhem et al., 2020a). For a latent variable model for data $\mathbf{x} \in \mathcal{X}$ with latents $\mathbf{z} \in \mathcal{Z}$, the definition of identifiability is:

Definition 1 (Identifiability up to equivalence class, Khemakhem et al. (2020a)).

Let \sim be an equivalence relation on Θ . A model defined by $p_\theta(\mathbf{x}, \mathbf{z}) = p_\theta(\mathbf{x}|\mathbf{z})p_\theta(\mathbf{z})$ with $\theta \in \Theta$ is said to be identifiable up to \sim if $p_\theta(\mathbf{x}) = p_{\theta'}(\mathbf{x}) \rightarrow \theta \sim \theta'$. The elements of the quotient space Θ / \sim are called the identifiability classes.

In this approach, identifiability comes from *conditional priors* – the latents $\mathbf{z} \in \mathcal{Z} = \mathbb{R}^{d_z}$ in the generative model are themselves conditioned on the same kinds of auxiliary information $\mathbf{u} \in \mathcal{U}$ as used in the constrastive method. The priors must have the form

$$p_\theta(\mathbf{z}|\mathbf{u}) = \prod_{i=1}^{d_z} \frac{Q_i(z_i)}{Z_i(\mathbf{u})} \exp \left[\sum_{j=1}^k T_{i,j}(z_i) \lambda_{i,j}(\mathbf{u}) \right], \quad (1)$$

where $T_{i,j}$ are the sufficient statistics of the distribution, $\lambda_{i,j}$ its natural parameters with normaliser Z_i and base measure Q_i (commonly 1). k is the maximum order of statistics of these distributions. (For us $k = 2$ throughout as, following previous work, we choose $p_\theta(\mathbf{z}|\mathbf{u})$ to be a product of independent Gaussians.) The generative model must form a Bayes net $\mathbf{u} \rightarrow \mathbf{z} \rightarrow \mathbf{x}$, and $p_\theta(\mathbf{x}|\mathbf{z}) = p_\epsilon(\mathbf{x} - f_\theta(\mathbf{z}))$ for some noise ϵ . The equivalence relation for identifiability in this class of latent variable models is:

Proposition 1 (Equivalence \sim , Khemakhem et al. (2020a)).

$(f_\theta, \mathbf{T}, \lambda) \sim (\tilde{f}_\theta, \tilde{\mathbf{T}}, \tilde{\lambda})$ are of the same equivalence class if and only if there exist \mathbf{A} and \mathbf{c} such that $\forall \mathbf{x} \in \mathcal{X}$, $\mathbf{T}(f_\theta^{-1}(\mathbf{x})) = \mathbf{A}\tilde{\mathbf{T}}(\tilde{f}_\theta^{-1}(\mathbf{x})) + \mathbf{c}$.

Analogously to the contrastive case, the choice of \mathbf{u} -task is the choice of which unmixing you get – it is intrinsic in all these approaches that they provide identifiability up to the choice of \mathbf{u} -task. See Figure 1 for an example of different \mathbf{u} -tasks for an imagined dataset. That is, different \mathbf{u} -tasks cannot be expected to provide the same learnt, mutually identifiable representations as each other – after all, the representations are *for* a particular purpose, and that purpose is determined by the choice of \mathbf{u} -task. In order for the generative model to be identifiable, the \mathbf{u} -task has to follow certain mathematical constraints.

Theorem 1 (Identifiability Theorem, Khemakhem et al. (2020a)).

Suppose that: (i) The set $\{\mathbf{x} \in \mathcal{X} | \Psi_\epsilon(\mathbf{x}) = 0\}$ is of measure zero, where $\Psi_\epsilon(\mathbf{x})$ is the characteristic function of the noise density $p_\epsilon(\cdot)$; (ii) the mixing function f_θ is injective; (iii) The sufficient statistics $T_{i,j}$ in Eq (1) are differentiable almost everywhere and $T'_{i,j} = 0$ almost everywhere for $i \in \{1, \dots, d_z\}$ and $j \in \{1, \dots, k\}$; (iv) There exist $(kd_z + 1)$ distinct values of \mathbf{u} , $\mathbf{u}_0, \dots, \mathbf{u}_{(k \times d_z) + 1}$, such that the following $kd_z \times kd_z$ matrix is invertible:

$$\mathbf{L} = (\boldsymbol{\lambda}(\mathbf{u}_1) - \boldsymbol{\lambda}(\mathbf{u}_0), \dots, \boldsymbol{\lambda}(\mathbf{u}_{kd_z+1}) - \boldsymbol{\lambda}(\mathbf{u}_0)). \quad (2)$$

Thus in this approach the theory of non-linear ICA is linked to the theory of deep generative models. When this theory is applied to VAEs one gets Identifiable-VAEs (iVAEs) (Khemakhem et al., 2020a). For iVAEs the ELBO, for a single datapoint \mathbf{x} and its associated auxiliary \mathbf{u} , is

$$p(\mathbf{x}|\mathbf{u}) \geq \mathcal{L}^{\text{iVAE}}(\mathbf{x}|\mathbf{u}; \theta, \phi) = \mathbb{E}_{q_\phi(\mathbf{z}|\mathbf{x}, \mathbf{u})} \log p_\theta(\mathbf{x}|\mathbf{z}) - \text{KL}[q_\phi(\mathbf{z}|\mathbf{x}, \mathbf{u}) || p_\theta(\mathbf{z}|\mathbf{u})]. \quad (3)$$

For this identifiability theory to hold for iVAEs: the generative model must be an infinitely-flexible function-approximator; the true posterior has to be in the family of q posteriors; we must have infinite data; and the maximum value of $\mathcal{L}^{\text{iVAE}}$ must be found during optimisation (Khemakhem et al., 2020a). The conditional priors in \mathcal{Z} can be implemented as Gaussians, $p_\theta(\mathbf{z}|\mathbf{u}) = \mathcal{N}(\mathbf{z}|\boldsymbol{\mu}_\theta(\mathbf{u}), \boldsymbol{\Sigma}_\theta(\mathbf{u}))$ where $\boldsymbol{\mu}_\theta(\cdot)$ and $\boldsymbol{\Sigma}_\theta(\cdot)$ are themselves neural networks or look-up tables (and $\boldsymbol{\Sigma}_\theta(\cdot)$ must be diagonal to fulfill Eq (1)).

3. Identifiable Non-Linear ICA via Clustering

Here we flip the perspective of having \mathbf{u} as data, instead aiming to jointly learn \mathbf{u} along with \mathbf{z} . We will consider each parameterisation of a deep generative model with structure $\mathbf{u} \rightarrow \mathbf{z} \rightarrow \mathbf{x}$ as implicitly inducing a particular \mathbf{u} -task, towards which it is identifiable. Recall that \mathbf{u} is used in the iVAE context to index over different priors in the latent space \mathbf{z} . That is, there is a set of distributions $\{p_\theta(\mathbf{z}|\mathbf{u})\}$ for $\mathbf{u} \in \mathcal{U}$. In the iVAE setting our data is composed of $\{\mathbf{x}, \mathbf{u}\}$ pairs. In prior work when training on standard datasets the class index is used as \mathbf{u} .

Instead of having these \mathbf{u} labels given to us as data, our key idea is to obtain our \mathbf{u} values from learning a clustering of our data. We will learn our clustering jointly with learning the (identifiable) representation \mathbf{z} , in a fully probabilistic and unified manner.

For iVAEs, having access to true values of \mathbf{u} is equivalent to having a posterior for \mathbf{u} that is one-hot, deterministic. We relax this assumption, aiming to jointly learn both the \mathbf{u} -task and \mathbf{u} posteriors as we learn our \mathbf{z} posteriors and the rest of the generative model. Thus we have changed the problem to a form of clustering – \mathbf{u} is the learnt clustering index in the latent space. The structure of the learnt \mathbf{u} will emerge as a natural consequence of the representational power of the model. For example, a model with single-layer linear mappings will naturally learn very different representations to a model with multiple convolutional layers trained on the same dataset.

Our claim is that the same DGM clustering architecture will learn highly-similar \mathbf{u} representations when retrained with different initialisations and thus lead to consistently-learnt \mathbf{z} representations when the model is retrained on the same dataset. What representations the model learns, what \mathbf{u} -task, is a result of the interactions between the model’s particular inductive biases and the dataset being trained on. From this reproducible \mathbf{u} -clustering being learnt, we can then apply the results from the previous theoretical work, described above, that proves that conditional-prior DGM models are identifiable. In our experimental results we find, for various datasets, that the learnt representations of our clustering approach, where \mathbf{u} is learnt, are identifiable.

Critically, we do not need our model to naturally cluster into any particular pre-specified \mathbf{u} -tasks – we are leveraging the theoretical insight in (Khemakhem et al., 2020a) that there is a whole world of \mathbf{u} -tasks that provide sufficient separation to obtain identifiability. In particular we are *not* aiming to match the ground-truth class labels, for example, that are given with standard datasets. Instead, we observe that deep generative models with latent mixtures naturally learn clusterings that correspond to appropriate, sufficient \mathbf{u} -tasks. (For an intuitive example of this, see Figure 1.) Here we bring together these ideas to demonstrate the empirical identifiability of latent representations in deep clustering models, which implicitly perform non-linear ICA.

We wish to underline that we in no way dispute previous results on the impossibility of generic, unique non-linear ICA. Rather we are saying that, for finitely-expressive models their particular capacity induces a natural emergent clustering in their latent space from which we can obtain identifiable representations. We highlight that theoretical results (Hyvärinen & Morioka, 2016; Hyvarinen et al., 2019; Khemakhem et al., 2020a) assume universal function approximators. If our models were infinitely flexible then our approach would indeed fail.

The ELBO for an iVAE, Eq (3), can be re-written, so that instead of having our log evidence conditioned on \mathbf{u} we have it as a latent variable, albeit one with a one-hot posterior,

$$\mathcal{L}^{\text{iVAE}}(\mathbf{x}|\mathbf{u}; \theta, \phi) = \mathcal{L}^{\text{iVAE}}(\mathbf{x}; \theta, \phi) = \mathbb{E}_{q_\phi(\mathbf{u}|\mathbf{x})} \left[\mathbb{E}_{q_\phi(\mathbf{z}|\mathbf{x}, \mathbf{u})} \log p_\theta(\mathbf{x}|\mathbf{z}) - \text{KL}(q_\phi(\mathbf{z}|\mathbf{x}, \mathbf{u})||p_\theta(\mathbf{z}|\mathbf{u})) \right]. \quad (4)$$

where $q_\phi(\mathbf{u}|\mathbf{x}) = \delta(\mathbf{u} - \omega(\mathbf{x}))$ is the deterministic distribution that maps perfectly from each \mathbf{x} to its associated \mathbf{u} , returned by $\omega(\mathbf{x})$. In the standard iVAE setting, $q_\phi(\mathbf{u}|\mathbf{x})$ is implemented using a lookup-table – we are told the true values of \mathbf{u} for each datapoint \mathbf{x} .

We relax the assumption that $q_\phi(\mathbf{u}|\mathbf{x})$ has to be given externally. Instead, we leverage the intrinsically-limited representational power of our chosen model. Whatever clustering is naturally learnt by our q networks defines our \mathbf{u} variables – it is simply the clustering variable learnt by our model.

Now \mathbf{u} is simply an additional latent variable, a discrete latent over cluster components in \mathcal{Z} . This means we will perform inference over it, having placed a prior over it. This means our generative model is $p_\theta(\mathbf{x}|\mathbf{z})p_\theta(\mathbf{z}|\mathbf{u})p_\theta(\mathbf{u})$. For inference we use the approach first proposed in VaDE¹ (Jiang et al., 2017).

1. Recently (Falck et al., 2021) has corrected some mistakes in the original VaDE paper, but interestingly these mistakes only become apparent when using more than one Monte Carlo sample $\mathbf{z} \sim q_\phi(\mathbf{z}|\mathbf{x})$ when estimating \mathcal{L} . We use one such sample, as is common practice regardless. Our description of VaDE reflects the corrections made in (Falck et al., 2021).

In this approach one makes two design choices. First, choose the factorisation $q_\phi(\mathbf{z}, \mathbf{u}|\mathbf{x}) = q_\phi(\mathbf{z}|\mathbf{x})q_\phi(\mathbf{u}|\mathbf{x})$. Writing the generative model as $p_\theta(\mathbf{x}|\mathbf{z})p_\theta(\mathbf{z})p_\theta(\mathbf{u}|\mathbf{z})$, we can write the ELBO as

$$\mathcal{L}^{\text{VaDE}}(\mathbf{x}; \theta, \phi) = \mathbb{E}_{q_\phi(\mathbf{z}|\mathbf{x})} \log p_\theta(\mathbf{x}|\mathbf{z}) - \text{KL}[q_\phi(\mathbf{z}|\mathbf{x})||p_\theta(\mathbf{z})] - \mathbb{E}_{q_\phi(\mathbf{z}|\mathbf{x})} \text{KL}[q_\phi(\mathbf{u}|\mathbf{x})||p_\theta(\mathbf{u}|\mathbf{z})]. \quad (5)$$

The second design choice is choosing to parameterise $q_\phi(\mathbf{u}|\mathbf{x})$ not using its own, additional, recognition network. Instead one constructs the Bayes-optimal posterior for our chosen q -factorisation: the $q_\phi(\mathbf{u}|\mathbf{x})$ that minimises $\mathbb{E}_{q_\phi(\mathbf{z}|\mathbf{x})} \text{KL}(q_\phi(\mathbf{u}|\mathbf{x})||p(\mathbf{u}|\mathbf{z}))$. This is the case when $q_\phi(\mathbf{u}|\mathbf{x}) \propto \exp(\mathbb{E}_{q_\phi(\mathbf{z}|\mathbf{x})} \log p_\theta(\mathbf{u}|\mathbf{z}))$ (Falck et al., 2021).

When estimating \mathcal{L} using a single sample $\mathbf{z} \sim q_\phi(\mathbf{z}|\mathbf{x})$ and constructing $q_\phi(\mathbf{u}|\mathbf{x})$ using that sample, the Monte Carlo (MC) estimate of $\mathbb{E}_{q_\phi(\mathbf{z}|\mathbf{x})} \text{KL}[q_\phi(\mathbf{u}|\mathbf{x})||p_\theta(\mathbf{u}|\mathbf{z})]$ is zero (Falck et al., 2021). This further simplifies optimisation, giving us our single-MC-sample estimator for $\mathcal{L}^{\text{VaDE}}$,

$$\mathcal{L}_{\text{MC}}^{\text{VaDE}}(\mathbf{x}; \theta, \phi) = \mathbb{E}_{q_\phi(\mathbf{z}|\mathbf{x})} \log p_\theta(\mathbf{x}|\mathbf{z}) - \text{KL}[q_\phi(\mathbf{z}|\mathbf{x})||p_\theta(\mathbf{z})]. \quad (6)$$

Overall this approach has numerous benefits. Firstly, with it we do not have to perform expensive exact marginalisation over the discrete latent. In some models each possible value of the discrete latent requires a forward pass through a neural network. Secondly, we do not have to use the Gumbel-Softmax trick to get reparameterised samples from a relaxed discrete distribution, which would introduce bias. As a result, this approach admits a simple, lightweight, stochastic estimator over minibatches of data. Finally, in this work we are particularly interested in the intrinsic identifiability of the model we are training. Each additional neural component introduced requires its own design choices that in turn will affect the inductive bias of the overall model. With this approach, we end up training a vanilla VAE but for the fact that we have a learnt Gaussian Mixture Model as the prior in \mathcal{Z} . We study the effect of different design choices for p and q in the next section in more detail. Further, see Appendix for experiments with a randomly-sampled and then fixed amortised posterior for \mathbf{u} .

Enforcing requirements for identifiability Identifiability in iVAEs is obtained when the matrix \mathbf{L} , Eq (2), made out of the natural parameters of our conditional priors $\{p_\theta(\mathbf{z}|\mathbf{u})\}$, is invertible. Optimising the ELBO of our clustering models while ensuring that this is the case means our problem is one of constrained optimisation. We can thus use an approach reminiscent of projected gradient descent (Beck, 2017). We simply track the invertibility of \mathbf{L} during optimisation and if it becomes uninvertible we can add a small amount of noise to the natural parameters of the conditional priors². However, we found empirically that this process was not invoked – the constraint on the mixture model’s parameters is sufficiently easy to satisfy that, when simply optimising $\mathcal{L}^{\text{VaDE}}$, \mathbf{L} remains invertible.

Recall that in order to construct \mathbf{L} there have to be $(k \times d_z) + 1$ different values of \mathbf{u} and for Gaussians $k = 2$. When using standard image datasets, the ground-truth class labels provide a natural \mathbf{u} -task. For many datasets (SVHN, CIFAR10, MNIST, etc), there are 10 classes. This means that under the terms of this identifiability theory, an iVAE with Gaussian $p_\theta(\mathbf{z}|\mathbf{u})$ distributions trained on these datasets can have at most $d_z = 4$. Yet already the ideas underpinning iVAEs have been extended to flows, where $d_z = d_x$ by construction, and have been found to work (Sorrenson et al., 2020). Empirically, it thus seems that the requirement of \mathbf{L} invertibility is a sufficient but not necessary condition. To that end, in our empirical investigations we do not constrain the latent spaces of our models to be so small, and we find that iVAEs, and our clustering approach, produce identifiable models even with $d_z = 200$ – for which \mathbf{L} is not even possible to construct.

2. Alternatively, one could view this as a soft constraint, and so add an additional term to the objective that captures the invertibility of \mathbf{L} . The Condition Number, $\text{CN}(\cdot)$, would be one way to do this: $\tilde{\mathcal{L}} = \mathcal{L} - \alpha \text{CN}(\mathbf{L})$.

4. Experiments

We will train iVAEs and VaDEs on both synthetic data and standard image datasets. For us two questions naturally emerge. The first, applicable to synthetic data where the true generative factors are known, is: *does our clustering approach produce identifiable models in terms of discovering the true sources underpinning a dataset, benchmarked against iVAEs?* The second, applicable to training on image datasets, is: *do reruns of the same VaDE model result empirically in identifiable latent representations, benchmarked against iVAEs?* We will answer these in turn.

For our runs we measured the mean correlation coefficient (MCC) between the learnt latents and ground-truth sources, for synthetic data where we have access to the true generative factor, and between pairs of learnt latents from models trained with different seeds when we train on standard datasets (for which we do not have access to the ground-truth sources). Large MCC indicates strong correlation between inputs, be it between the latents recovered and the true sources or two sets of latents learnt with different seed.

4.1 Synthetic Data

We create synthetic data to evaluate model performance using the same generating mechanism and mode of analysis as in previous in works on non-linear ICA (Hyvärinen & Morioka, 2016; Hyvarinen et al., 2019; Khemakhem et al., 2020a; Sorrenson et al., 2020; Li et al., 2020; Khemakhem et al., 2020b). We generate Time-Contrastive Learning data with $d_x = d_z = 5$, constructing data in 20 segments. Each segment’s data is made by sampling from a random product of Gaussians with means with uniformly distributed on $[-3, 3]$ and standard deviations uniformly distributed on $[0.01, 3]$. These sources were mixed by a 4-layer random MLP, where the weight matrices were constructed to be full-rank, with LeakyRelu activations functions. We constructed five different datasets, varying by the number of samples per segment in $\{100, 200, 500, 1000, 2000\}$.

We trained iVAE and VaDE models 10 times with different seeds on these five datasets, with iVAEs and VaDEs using the same neural architectures as each other for both the encoder and decoder. For both networks we used 3-layer MLPs with LeakyRelu activations functions and trained using ADAM (Kingma & Lei Ba, 2015) for 70,000 steps, with an initial learning rate of 0.001 that we decay on plateau. For VaDE $p_\theta(\mathbf{z})$ is a 40-component Gaussian mixture model, with the means and log variances Xavier-uniformly initialised (Glorot & Bengio, 2010).

We show boxplots of the resulting MCC values, Figure 2. We find that VaDE achieves MCC results that are as high or higher than iVAE does, indicating that it is as successful or more successful at discovering the true latents as iVAE is.

We can also ask, is model quality, as measured by \mathcal{L} on the training data, a predictor of successful non-linear un-mixing in VaDE models on this task? We plot \mathcal{L} against MCC for VaDE, Figure 3, and find that yes \mathcal{L} and MCC are positively correlated.

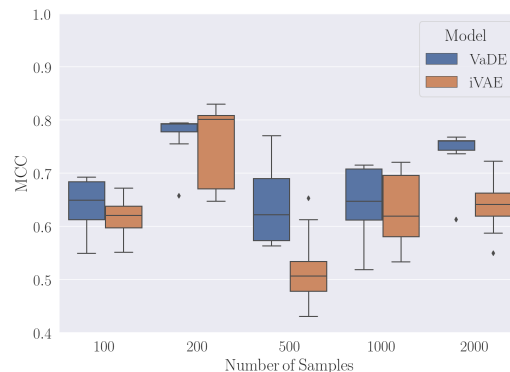


Figure 2: MCC for VaDE and iVAE for synthetic data generated using $L = 4$ mixing layers.

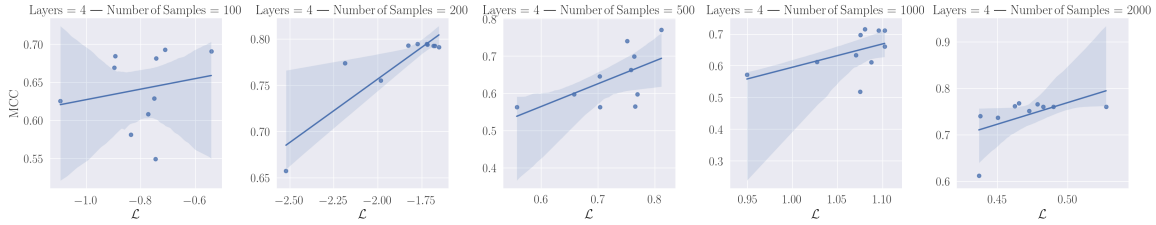


Figure 3: MCC (to ground-truth sources) as a function of \mathcal{L} for VaDE models trained on synthetic data, for five different datasets of different sizes. Different points correspond to different random restarts. Shading is over the 95% confidence interval.

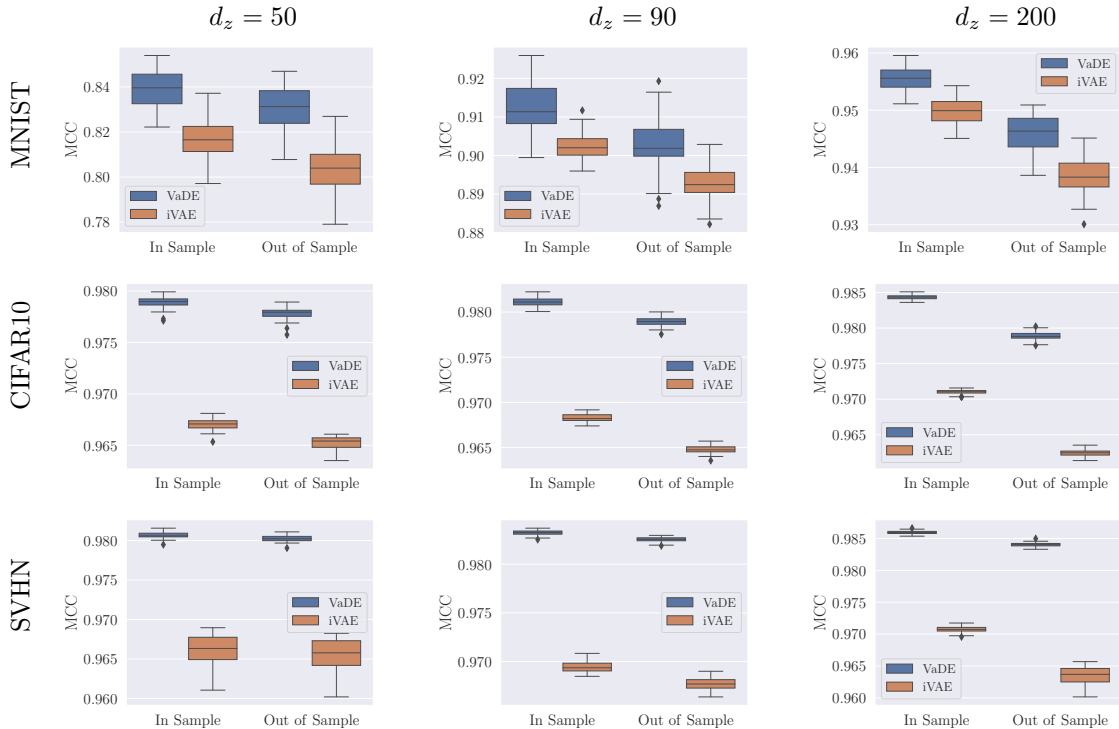


Figure 4: Plots showing the linear identifiability of $\mu_\phi(\mathbf{x})$ for MLP models with $d_z \in \{50, 90, 200\}$ as measured by MCC. We trained each model- d_z -dataset combination 10 times with different seeds. We used half of the test set to find the best linear mapping \mathbf{A} between between representations for each pair of seeds. We do this alignment using Canonical Correlation Analysis (CCA) (Hotelling, 1936). We show MCC values of the aligned spaces over the test set for both ‘in sample’ (MCC calculated over the half of the test set \mathbf{z} values used to find the CCA mapping) and ‘out of sample’ (MCC calculated over the remaining \mathbf{z} values). VaDE, the purely unsupervised clustering approach, is in all cases scores about as well as iVAE, which is given a ground-truth \mathbf{u} value, or better. Note that y-axes vary in scale.

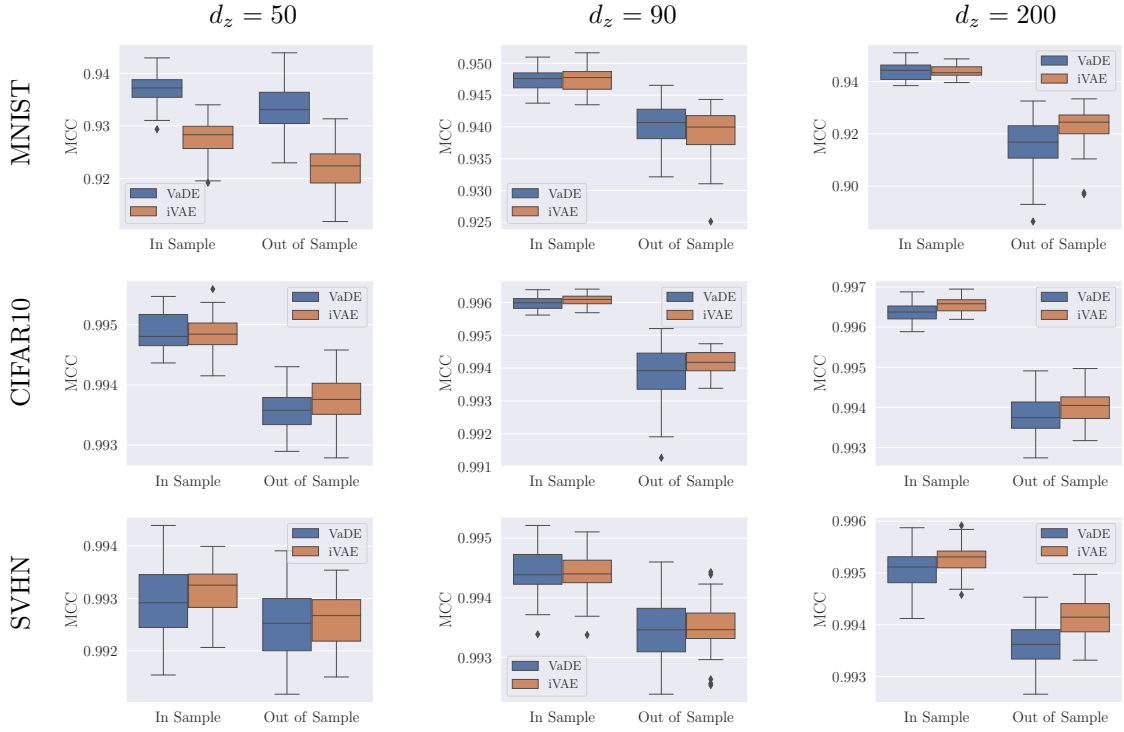


Figure 5: Plots showing the linear identifiability of $\mu_\phi(\mathbf{x})$ for ConvNet models with $d_z \in \{50, 90, 200\}$ as measured by MCC. The overall method of analysis is the same as for MLP results. VaDE, the purely unsupervised clustering approach, in all cases scores about as well as iVAE, which is given a ground-truth \mathbf{u} value. Note that y-axes vary in scale.

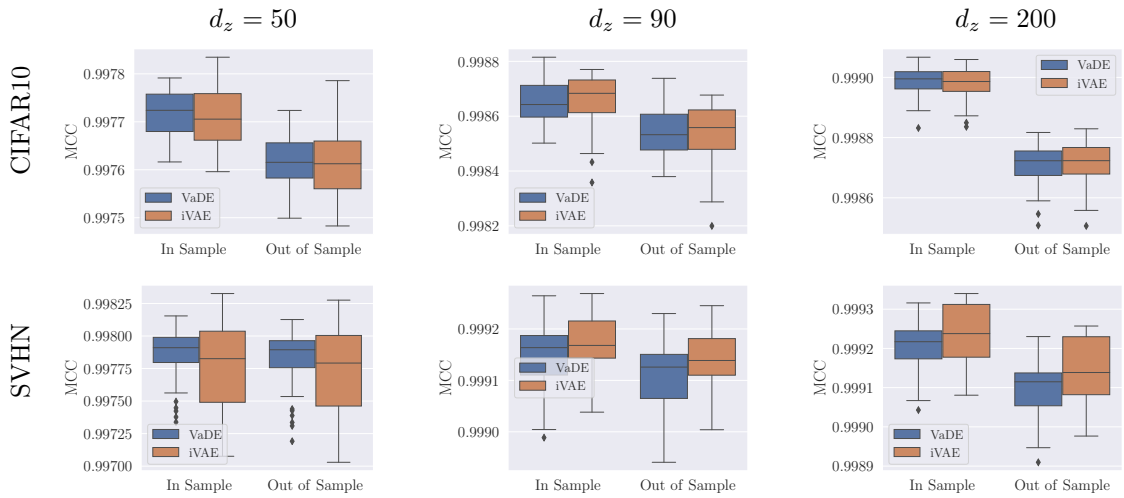


Figure 6: Plots showing the linear identifiability of $\mu_\phi(\mathbf{x})$ ResNet models with $d_z \in \{50, 90, 200\}$ as measured by MCC. The overall method of analysis is the same as for MLP and ConvNet results. VaDE, the purely unsupervised clustering approach, in all cases scores about as well as iVAE, which is given a ground-truth \mathbf{u} value. Note that y-axes vary in scale.

4.2 Image Data

We are particularly interested in the identifiability of VaDE, benchmarked against iVAE, when trained on standard image datasets and over a range of neural architectures. We train iVAE and VaDE with the encoders and decoders being MLPs, ConvNets and ResNets. With these architectures we are trying to capture a range of model richness and representational power. See Appendix for detailed descriptions of the neural architectures. We trained 480 DGMs for the experiments in this section³.

For each model-architecture-dataset combination we train $d_z \in \{50, 90, 200\}$, and for each of these we train with 10 different seeds. We train on MNIST, CIFAR10 and SVHN. For iVAE, we use the provided class label as \mathbf{u} ; for VaDE we introduce a 40-component mixture model for MNIST and a 100-component mixture models for CIFAR-10 and SVHN.

We wish to underline that we carried out no architecture tuning or tuning of optimisation method, beyond finding a learning rate that provided stable optimisation in terms of training set \mathcal{L} . Rather we implemented three architectures for VAEs and trained them, as iVAEs and VaDEs. The idea in these experiments is not to tune some lucky architecture that happens to lead to consistently-learned representations, but to demonstrate the robustness of our VaDE-unmixing (and iVAE-unmixing) to different neural parameterisations. All training was done with a batch size of 64 using ADAM. We had to make small changes to the models to handle different datasets: 1) those needed to handle $28 \times 28 \times 1$ images (MNIST) vs $32 \times 32 \times 3$ images (CIFAR10 and SVHN) and 2) the choice of likelihood function, Bernoulli for MNIST and Logistic (Kingma et al., 2016, §C.5) for CIFAR10 and SVHN.

As we do not have recorded the true underlying latent sources that generated these images, in order to evaluate these models we follow (Khemakhem et al., 2020b) in measuring the MCC between matching runs with different seeds. For 10 different random restarts we get 55 pairs of seeds. We show the results for VaDE and iVAE in Figures 4-6. For MLPs, VaDE consistently reaches higher MCC values than iVAEs do. For ConvNets and ResNets, performance is very similar between VaDE and iVAE.

The results we show indicates that, even though VaDE is trained unsupervised, it naturally learns repeatable representations of data, across a range of datasets and model architectures. Empirically this leads to identifiability, as measured by MCC. As well as providing empirical evaluation of our ideas, this is also the first large-scale evaluation of the identifiability of iVAEs on image data.

Limitations While we show experimental verification of our ideas, the idea of replacing a fixed and given set of \mathbf{u} values with a set that is obtained via the natural partitions learnt in the latent space of a model requires that that partitioning is identifiable. We have given a large amount of experimental evidence, but always it is desirable to have more. In the main experimental results, on image data, we have covered three different neural parameterisations: MLPs, ConvNets and ResNets. Within each of these there are more variations to consider, different numbers of filters in the convolutional layers, say; there are also other possible parameterisations one could consider. Further, formal analysis of the conditions necessary for consistently-learned partitioning of the latent space in parametric generative models is not a part of this paper, and would be of great value to the field.

5. Related Work

Our discussion of the range of potential \mathbf{u} -tasks in the context of non-linear ICA is mirrored in the deep clustering literature, that for a given dataset there are multiple ways that one could plausibly cluster the data (Li et al., 2019; Willetts et al., 2019; Falck et al., 2021). For instance, for MNIST one might aim to cluster over digit identity, but also one could aim to cluster over stroke thickness,

3. With each run taking on average ~ 8 h on an M60 GPU, this means that if performed in series these experiments would take ~ 5 months.

or the left-right slant of the written digits, or some more baroque task like how many genera (in a topological sense) each written digit contains. (This last task would, for instance, separate the two ways of writing '4's.)

This phenomena, that different clustering algorithms lead to different natural clusterings of the data, has been discussed in the context of semi-supervised learning (Nigam et al., 2000; Corduneanu & Jaakkola, 2002). This is a problem in this setting, as the additional unlabelled data can then degrade rather than improve classification performance. In terms of Figure 1, the situation would be having a small amount of data annotated with the shape of objects, say, but a model that naturally partitions over colour. For us, however, any informative clustering of the data serves our purposes as long as it is consistently learnt by the model and fulfills the technical requirements of (Khemakhem et al., 2020a).

As mentioned above, classifier-based approaches to non-linear ICA (Hyvärinen & Morioka, 2016; Hyvarinen et al., 2019) are the cousins of contrastive methods for self-supervised learning (Gutmann & Hyvärinen, 2012; Oord et al., 2018; Henaff et al., 2020; He et al., 2020). The \mathbf{u} -tasks used in the context of non-linear ICA are exactly the tasks one can use in contrastive self-supervised learning, and vice versa. Examples include, separating the channels of colour images and aiming to match the pair of different channels that came from the same image (Oord et al., 2018), or matching different modalities or augmentations of the same datapoint (Wu et al., 2018; Bachman et al., 2019; Chen et al., 2020; He et al., 2020). See (Tian et al., 2020) for a recent analysis of what makes a good \mathbf{u} -task in contrastive learning. Further, the connection between contrastive learning and classifier-based methods to non-linear ICA has been formalised in the 'Incomplete Rosetta stone problem' (Gresele et al., 2020).

There is a strand, also, of self-supervised learning that aims to learn a clustering over the data simultaneously with the representations (Yang et al., 2016; Caron et al., 2018; Huang et al., 2019; Zhuang et al., 2019; Asano et al., 2020; Caron et al., 2020). These approaches so far are mostly theoretically-distinct from contrastive methods (though (Caron et al., 2020) is perhaps the start of a unification). We think that the two lenses we explore, clustering DGMs and non-linear ICA, might provide a way for the two self-supervised approaches of clustering and contrastive methods to be unified. Finally, recently work has been done that explicitly aims to learn two representations simultaneously where the objective is to minimise the cross-correlation between the pair of representations (Zbontar et al., 2021; Bardes et al., 2021), which is done in our work and others (Khemakhem et al., 2020b) using linear canonical-correlation analysis to find alignment (prior to calculating MCC values) between the representations of random restarts of a model.

6. Conclusion

Here we have shown how DGMs combined with learnt clustering of their latent space can provide identifiable representations, scoring similarly to or better than iVAEs in terms of MCC values, across a range of datasets and neural parameterisations. This work in no way questions the result that non-linear ICA is impossible to perform in general when using infinite-capacity models (Hyvärinen & Pajunen, 1999). Rather we are observing that the inductive biases of DGMs are sufficient to induce clustering in their latent representation that itself is sufficiently consistent run-to-run to be used to apply the theory of iVAEs. This work opens the question of when our parametric, finite, models are identifiable in practice.

References

- Achlioptas, D. (2003). Database-friendly random projections: Johnson-Lindenstrauss with binary coins. In *Journal of Computer and System Sciences*, volume 66 (pp. 671–687).
- Asano, Y. M., Rupprecht, C., & Vedaldi, A. (2020). Self-labelling via simultaneous clustering and representation learning. In *ICLR*.
- Bachman, P., Devon Hjelm, R., & Buchwalter, W. (2019). Learning representations by maximizing mutual information across views. In *NeurIPS*.
- Bardes, A., Ponce, J., & LeCun, Y. (2021). VICReg: Variance-Invariance-Covariance Regularization for Self-Supervised Learning. *arXiv preprint*.
- Beck, A. (2017). *First-order methods in optimization*. SIAM.
- Bishop, C. M. (2006). *Pattern Recognition and Machine Learning*. New York.
- Camuto, A., Willetts, M., Paige, B., Holmes, C., & Roberts, S. (2021). Learning Bijective Feature Maps for Linear ICA. In *AISTATS*.
- Caron, M., Bojanowski, P., Joulin, A., & Douze, M. (2018). Deep clustering for unsupervised learning of visual features. In *Proc. ECCV*.
- Caron, M., Misra, I., Mairal, J., Goyal, P., Bojanowski, P., & Joulin, A. (2020). Unsupervised Learning of Visual Features by Contrasting Cluster Assignments. In *NeurIPS*.
- Chen, R., Li, X., Grosse, R., & Duvenaud, D. (2018). Isolating Sources of Disentanglement in Variational Autoencoders. In *NeurIPS*.
- Chen, T., Kornblith, S., Norouzi, M., & Hinton, G. (2020). A simple framework for contrastive learning of visual representations. In *ICML*.
- Corduneanu, A. & Jaakkola, T. (2002). Continuation Methods for Mixing Heterogenous Sources. In *UAI* (pp. 111–118).
- Dasgupta, S. & Gupta, A. (2003). An Elementary Proof of a Theorem of Johnson and Lindenstrauss. *Random Structures and Algorithms*, 22(1), 60–65.
- Esmaili, B., Wu, H., Jain, S., Bozkurt, A., Siddharth, N., Paige, B., Brooks, D. H., Dy, J., & van de Meent, J.-W. (2019). Structured Disentangled Representations. In *AISTATS*.
- Falck, F., Zhang, H., Willetts, M., Nicholson, G., Yah, C., & Holmes, C. (2021). Multi-Facet Clustering Variational Autoencoders. *arXiv preprint*.
- Glorot, X. & Bengio, Y. (2010). Understanding the difficulty of training deep feedforward neural networks Xavier. In *AISTATS*.
- Gresele, L., Rubenstein, P. K., Mehrjou, A., Locatello, F., & Schölkopf, B. (2020). The Incomplete Rosetta Stone Problem: Identifiability results for multi-view nonlinear ICA. In *AISTATS*.
- Gutmann, M. U. & Hyvärinen, A. (2012). Noise-contrastive estimation of unnormalized statistical models, with applications to natural image statistics. *Journal of Machine Learning Research*, 13, 307–361.
- Hastie, T., Tibshirani, R., & Friedman, J. (2017). *The Elements of Statistical Learning Data*.
- He, K., Fan, H., Wu, Y., Xie, S., & Girshick, R. (2020). Momentum Contrast for Unsupervised Visual Representation Learning. In *CVPR*.

- Henaff, O. J., Srinivas, A., Fauw, J. D., Razavi, A., Doersch, C., Eslami, S. M., & Eslami, A. V. O. (2020). Data-Efficient image recognition with contrastive predictive coding. *ICML*.
- Higgins, I., Matthey, L., Pal, A., Burgess, C., Glorot, X., Botvinick, M., Mohamed, S., & Lerchner, A. (2017). β -VAE: Learning Basic Visual Concepts with a Constrained Variational Framework. In *ICLR*.
- Hotelling, H. (1936). Relations Between Two Sets of Variates. *Biometrika*, 28(3/4), 321–377.
- Huang, J., Dong, Q., Gong, S., & Zhu, X. (2019). Unsupervised deep learning by neighbourhood discovery. In *ICML*.
- Hyvärinen, A. & Morioka, H. (2016). Unsupervised feature extraction by time-contrastive learning and Nonlinear ICA. *NeurIPS*.
- Hyvärinen, A. & Pajunen, P. (1999). Nonlinear independent component analysis: Existence and uniqueness results. *Neural Networks*, 12(3), 429–439.
- Hyvarinen, A., Sasaki, H., & Turner, R. E. (2019). Nonlinear ICA Using Auxiliary Variables and Generalized Contrastive Learning. In *AISTATS*.
- Jiang, Z., Zheng, Y., Tan, H., Tang, B., & Zhou, H. (2017). Variational Deep Embedding: An Unsupervised and Generative Approach to Clustering. In *IJCAI*.
- Johnson, W. B. & Lindenstrauss, J. (1984). Extensions of Lipschitz mappings into a Hilbert space. *Contemporary mathematics*, 26(1), 189–206.
- Khemakhem, I., Kingma, D. P., Monti, R. P., & Hyvärinen, A. (2020a). Variational Autoencoders and Nonlinear ICA: A Unifying Framework. In *AISTATS*.
- Khemakhem, I., Monti, R. P., Kingma, D. P., & Hyvärinen, A. (2020b). ICE-BeeM: Identifiable conditional energy-based deep models. In *NeurIPS*.
- Kim, H. & Mnih, A. (2018). Disentangling by Factorising. In *NeurIPS*.
- Kingma, D. P. & Lei Ba, J. (2015). Adam: A Method for Stochastic Optimisation. In *ICLR*.
- Kingma, D. P., Salimans, T., Jozefowicz, R., Chen, X., Sutskever, I., & Welling, M. (2016). Improved Variational Inference with Inverse Autoregressive Flow. In *NeurIPS*.
- Kingma, D. P. & Welling, M. (2014). Auto-encoding Variational Bayes. In *ICLR*.
- Li, S., Hooi, B., & Lee, G. H. (2020). Identifying through flows for recovering latent representations. In *ICLR*.
- Li, X., Chen, Z., Poon, L. K., & Zhang, N. L. (2019). Learning latent superstructures in variational autoencoders for deep multidimensional clustering. In *ICLR*.
- Locatello, F., Bauer, S., Lucie, M., Rätsch, G., Gelly, S., Schölkopf, B., & Bachem, O. (2019). Challenging common assumptions in the unsupervised learning of disentangled representations. In *ICML*, volume 2019-June.
- MacQueen, J. (1967). Some methods for classification and analysis of multivariate observations. In *Proceedings of the Fifth Berkeley Symposium on Mathematical Statistics and Probability, Volume 1: Statistics* (pp. 281–297): University of California Press.
- Nigam, K., McCallum, A. K., Thrun, S., & Mitchell, T. (2000). Text classification from labeled and unlabeled documents using EM. *Machine Learning*, 39(2), 103–134.

- Oord, A. v. d., Li, Y., & Vinyals, O. (2018). Representation Learning with Contrastive Predictive Coding. *arXiv preprint*.
- Oord, A. v. d., Vinyals, O., & Kavukcuoglu, K. (2017). Neural Discrete Representation Learning. *NeurIPS*.
- Papamakarios, G., Nalisnick, E., Rezende, D. J., Mohamed, S., & Lakshminarayanan, B. (2019). *Normalizing Flows for Probabilistic Modeling and Inference*. Technical report, DeepMind, London, UK.
- Rezende, D. J., Mohamed, S., & Wierstra, D. (2014). Stochastic Backpropagation and Approximate Inference in Deep Generative Models. In *ICML*.
- Roeder, G., Metz, L., & Kingma, D. P. (2021). On Linear Identifiability of Learned Representations. In *ICML*.
- Rolinek, M., Zietlow, D., & Martius, G. (2019). Variational autoencoders pursue pca directions (by accident). In *Proceedings of the IEEE Computer Society Conference on Computer Vision and Pattern Recognition*, volume 2019-June (pp. 12398–12407).
- Sønderby, C. K., Poole, B., & Mnih, A. (2017). Continuous Relaxation Training of Discrete Latent Variable Image Models. In *NeurIPS Bayesian Deep Learning Workshop*.
- Sorrenson, P., Rother, C., & Köthe, U. (2020). Disentanglement By Nonlinear ICA With General Incompressible-Flow Networks. *ICLR*.
- Tian, Y., Sun, C., Poole, B., Krishnan, D., Schmid, C., & Isola, P. (2020). What Makes for Good Views for Contrastive Learning? In *NeurIPS*.
- Tipping, M. E. & Bishop, C. M. (1999). Probabilistic Principal Component Analysis. *Journal of the Royal Statistical Society: Series B (Statistical Methodology)*, 61(3), 611–622.
- Willetts, M., Miscouridou, X., Roberts, S., & Holmes, C. (2020). Relaxed-Responsibility Hierarchical Discrete VAEs. *arXiv preprint*.
- Willetts, M., Roberts, S., & Holmes, C. (2019). Disentangling to Cluster: Gaussian Mixture Variational Ladder Autoencoders. In *NeurIPS Bayesian Deep Learning Workshop*.
- Woodruff, D. P. (2014). Sketching as a Tool for Numerical Linear Algebra. *Foundations and Trends in Theoretical Computer Science*, 10(2), 1–157.
- Wu, Z., Xiong, Y., Yu, S. X., & Lin, D. (2018). Unsupervised Feature Learning via Non-parametric Instance Discrimination. In *Proceedings of the IEEE Computer Society Conference on Computer Vision and Pattern Recognition* (pp. 3733–3742).
- Yang, J., Parikh, D., & Batra, D. (2016). Joint Unsupervised Learning of Deep Representations and Image Clusters. In *CVPR*.
- Zbontar, J., Jing, L., Misra, I., LeCun, Y., & Deny, S. (2021). Barlow Twins: Self-Supervised Learning via Redundancy Reduction. In *ICML*.
- Zhuang, C., Zhai, A., & Yamins, D. (2019). Local aggregation for unsupervised learning of visual embeddings. In *Proceedings of the IEEE International Conference on Computer Vision*.

Appendix for I Don't Need u: Identifiable Non-Linear ICA Without Side Information

Appendix A. Neural Network Architectures

Here we describe the neural network architectures used for our experiments. We include code to reproduce our experiments in the supplementary material.

We trained iVAEs and VaDEs on CIFAR10, SVHN and MNIST, using MLPs, ConvNets and ResNets for each of the encoder and decoder.

1. *MLP*: A series of fully connected layers, for encoder and decoder.
2. *ConvNet*: A series of convolutional layers followed by some fully connected layers for encoder. For decoder, some fully connected layers followed by a series of transposed convolutional layers.
3. *ResNet*: A series of downsampling ResNet blocks followed by some fully connected layers for encoder. For decoder, some fully connected layers followed by a series of upsampling ResNet blocks.

For detailed breakdowns of MLP architectures see Table [A.2], for ConvNets Table [A.3] and for ResNets Table [A.4]

For each neural parameterisation, we chose the dimensionality of the latent space d_z to be $\in \{50, 90, 200\}$, as discussed in the main paper. For both iVAEs and VaDEs we chose the set of conditionals $\{p_\theta(\mathbf{z}|\mathbf{u})\}_{\mathbf{u} \in \mathcal{U}}$ to be Gaussians with diagonal covariance.

In all experiments we trained using ADAM (Kingma & Lei Ba, 2015), with $(\beta_1, \beta_2) = (0.9, 0.999)$. We used mini-batches sizes of 64 in all runs, and we trained for 200 epochs, decaying learning rate on plateau. Our code is based on that included with papers (Khemakhem et al., 2020a,b), and is released under a GPL v3.0 license.

Table A.1: Dataset parameters

Sizes
Data: $d_x = w \times w \times n_c$
n_c : channels, w : width
MNIST: $n_c = 1, w = 28$
CIFAR10: $n_c = 3, w = 32$
SVHN: $n_c = 3, w = 32$

Table A.2: MLP Architecture in detail

Architecture	Layer Sequence
<i>MLP Encoder</i>	Input: $d_x = w \times w \times c$
	FC 512, LeakyReLU(0.1)
	FC 384, LeakyReLU(0.1)
	Dropout(0.1)
	FC 256, LeakyReLU(0.1)
	FC 256, LeakyReLU(0.1)
	$\mu_\phi(\mathbf{x})$: FC d_z
	$\sigma_\phi(\mathbf{x})$: FC d_z
<i>MLP Decoder</i>	Input: d_z
	FC 256, LeakyReLU(0.1)
	FC 256, LeakyReLU(0.1)
	Dropout(0.1)
	FC 384, LeakyReLU(0.1)
	FC 512, LeakyReLU(0.1)
	FC d_x

Table A.3: ConvNet Architecture in detail

Architecture	Layer Sequence	Notes
<i>ConvNet Encoder</i>	Input: $d_x = w \times w \times c$	stride 1 for convs, unless stated
	Conv $w \times w \times 8$, BatchNorm, ELU	padding 1, filter size 3
	Conv $w \times w \times 16$, BatchNorm, ELU	padding 1, filter size 3
	MaxPool $\frac{w}{2} \times \frac{w}{2} \times 16$	
	Conv $\frac{w}{2} \times \frac{w}{2} \times 32$, BatchNorm, ELU	padding 1, filter size 3
	Conv $\frac{w}{2} \times \frac{w}{2} \times 64$, BatchNorm, ELU	padding 1, filter size 3
	MaxPool $\frac{w}{4} \times \frac{w}{4} \times 64$	
	Conv $1 \times 1 \times 64$	padding 0, filter size $\frac{w}{4}$
	FC 64, LeakyReLU(0.1)	
	$\mu_\phi(\mathbf{x})$: FC d_z $\sigma_\phi(\mathbf{x})$: FC d_z	
<i>ConvNet Decoder</i>	Input: d_z	stride 1 for convs, unless stated
	FC 64, LeakyReLU(0.1)	
	FC 64	
	ConvTranspose $\frac{w}{4} \times \frac{w}{4} \times 64$, BatchNorm, ELU	padding 0, filter size $\frac{w}{4}$
	ConvTranspose $\frac{w}{2} \times \frac{w}{2} \times 32$, BatchNorm, ELU	padding 1, filter size 4, stride 2
	ConvTranspose $\frac{w}{2} \times \frac{w}{2} \times 16$, BatchNorm, ELU	padding 1, filter size 3
	ConvTranspose $w \times w \times 8$, BatchNorm, ELU	padding 1, filter size 4, stride 2
	Conv $w \times w \times c$	padding 1, filter size 3

Table A.4: ResNet Architecture in detail. ResNet blocks all have weightnorm applied to them, and in encoder downscale by a factor of 2 spatially, in the decoder they upscale by a factor of 2.

Architecture	Layer Sequence	Notes	
<i>ResNet Encoder</i>	Input: $d_x = w \times w \times c$	stride 1 for all conv. layers	
	Conv $w \times w \times 16$	padding 0, filter size 1	
	ResNet Block $\frac{w}{2} \times \frac{w}{2} \times 32$		
	ResNet Block $\frac{w}{4} \times \frac{w}{4} \times 64$		
	ResNet Block $\frac{w}{8} \times \frac{w}{8} \times 128$		
	ResNet Block $\frac{w}{16} \times \frac{w}{16} \times 256$		
	ResNet Block $\frac{w}{32} \times \frac{w}{32} \times 512$, ReLU		
	$\mu_\phi(\mathbf{x})$: FC d_z $\sigma_\phi(\mathbf{x})$: FC d_z		
	<i>ResNet Decoder</i>	Input: d_z	
		FC 512	
ResNet Block $\frac{w}{16} \times \frac{w}{16} \times 256$			
ResNet Block $\frac{w}{8} \times \frac{w}{8} \times 128$			
ResNet Block $\frac{w}{4} \times \frac{w}{4} \times 64$			
ResNet Block $\frac{w}{2} \times \frac{w}{2} \times 32$			
ResNet Block $w \times w \times 16$, ReLU			
Conv $w \times w \times c$	padding 0, filter size 1		

Appendix B. VQ-VAEs as Mixture models

There is another class of DGMs to which we can easily extend this analysis. Vector Quantised-VAEs (VQ-VAEs) (Oord et al., 2017) have a spatially-arrange grid of discrete latent variables (for images – for time series data a line would be used and for video a 3D block). These latent variables index over a shared codebook of embeddings. For each latent position the (deterministic) posterior is formed via an encoder that maps from inputs to the continuous space of the codebook vectors. The posterior over codebooks is simply defined to be one-hot on the closest codebook entry to the encoder’s embedding. As the lookup operation is not differentiable, an exponential moving average method with close links to K-means (MacQueen, 1967) is used to learn the codebook. VQ-VAEs are a kind of mixture model in disguise, with the learnt codebook embeddings acting as means.

While VQ-VAEs are deterministic models, as their posteriors over codebook indexes are one-hot, they do have a probabilistic relaxation (Sønderby et al., 2017), relaxed-VQ-VAEs (rVQ-VAEs). Here the posterior over codebook indexes is exactly the responsibilities used in learning a GMM using variational inference (Bishop, 2006, §10.2), albeit a mixture model where all components are hardcoded to have identity covariance.

We train relaxed-VQ-VAEs and a matching autoencoder baseline (where the continuous representations are directly given to the decoder, ie they are not quantised) 10 times each on CIFAR10 and measured the MCCs between the resulting \mathbf{z} representations. Of course the representations in these models form a grid, in the standard implementation we used⁴ this is an 8×8 grid, each entry in \mathbb{R}^{d_z} , so when calculating the MCC values we compare each latent grid position against its matching counterparts from other seeds. We then plot all these values, 8×8 latent positions $\times 55$ pairs of seeds from 10 restarts giving 3250 MCC values for each of rVQ-VAE and the baseline AE.

The rVQ-VAE is moderately higher in MCC than the AE baseline, but neither scores particularly high. So while explicitly having a mixture model in the latent representations does seem to increase MCC, it does not lead to the large values, often > 0.9 , seen for the iVAE and VaDE models we show in the main paper. This may be related to the fact that these rVQ-VAE and AE-baseline models have convolutional latents, so they are not parameterised by MLPs. Recall that the identifiability of iVAEs is, formally, only guaranteed when one has the dimensionality of the latent space sufficiently small. When one has a grid of spatially-arranged latents, as in these models, the effective latent dimensionality is much larger than for the models in the main paper. This might be part of the reason for the small MCC values. For a discussion of MLP vs convolutional (ie spatially-arranged) latents in VAEs, see (Willetts et al., 2020).

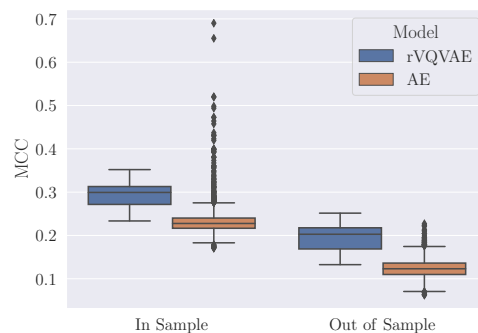


Figure B.1: MCC of rVQ-VAE vs baseline AE (where no quantisation is carried out) from 10 random restarts, trained on CIFAR10. Note that while it seems there are a lot of outliers for the AE baseline, recall that we are showing boxplots over 3250 MCC values for each model.

⁴ github.com/bshall/VectorQuantizedVAE

Appendix C. Rademacher-Hashed Posteriors for \mathbf{u}

In VaDE we learn our \mathbf{u} representations by learning to cluster our representations in \mathcal{Z} , learning both the \mathbf{z} and \mathbf{u} variables jointly. The posterior for \mathbf{u} is defined to be Bayes-optimal. However, one could define the posterior for \mathbf{u} in many different ways – using VaDE is a design choice we make, choosing it for both its naturalness and simplicity. In this section, we explore a method of defining $q_\phi(\mathbf{u}|\mathbf{x})$ using sketching/random projections/Johnson–Lindenstrauss (JL) transforms (Johnson & Lindenstrauss, 1984; Achlioptas, 2003; Dasgupta & Gupta, 2003; Woodruff, 2014) combined with simple hash.

We choose the number of cluster components, K , indexed by \mathbf{u} to be 2^N . We sample and then *fix* a simple random projection $\mathbf{A} \in \mathbb{R}^{N \times d_x}$ constructed from Rademacher random variables (Achlioptas, 2003) that projects from $\mathcal{X} = \mathbb{R}^{d_x}$ to \mathbb{R}^N :

$$A_{i,j} = \begin{cases} +1, & \text{with probability } \frac{1}{2} \\ -1, & \text{with probability } \frac{1}{2}. \end{cases} \quad (\text{C.1})$$

Let $\mathbf{h}(\mathbf{x}) = \mathbf{A}\mathbf{x}$, our JL embedding in \mathbb{R}^N . From this we can then define a binary representation \mathbf{b} of length N :

$$b_i(\mathbf{x}) = 0.5 \times (\text{sign}(h_i(\mathbf{x})) + 1). \quad (\text{C.2})$$

\mathbf{u} is then the one-hot representation of the binary vector \mathbf{b} :

$$\mathbf{u}^{\text{Rad}}(\mathbf{x}) = \text{onehot} \left(\sum_{i=0}^{N-1} 2^i \times b_i(\mathbf{x}) \right). \quad (\text{C.3})$$

The ‘posterior’ for \mathbf{u} is then simply this one-hot value: $q^{\text{Rad}}(\mathbf{u}|\mathbf{x}) = \delta(\mathbf{u} - \mathbf{u}^{\text{Rad}}(\mathbf{x}))$. While this construction is not differentiable, that is not important as we do not learn \mathbf{A} so no gradient propagation is needed.

This approach can be interpreted as constructing a Johnson-Lindenstrauss embedding out of \mathbf{x} of dimension N where which orthant a data point falls into in this JL-space is then used to index over mixture components in \mathcal{Z} , the latent space of our learnt DGM.

We train MLP mixture-model VAEs with 128 mixture components, so $N = 7$, on CIFAR10 with $d_z = 50$ using this JL-based construction, so $q_\phi(\mathbf{u}|\mathbf{x}) = q^{\text{Rad}}(\mathbf{u}|\mathbf{x})$, and a matching VaDE model as baseline, training each 10 times and measuring the MCC between pairs of runs as in the main paper. Each Rademacher-constructed run has differently-initiated \mathbf{A} projections – they are initiated using the same looped-over seed as all other neural network parameters in the model (though \mathbf{A} receives no updates, it is fixed).

We find that this method does lead to respectable MCC values, but it does not outperform directly learning to cluster in \mathcal{Z} , the approach that VaDE takes. We expect this is because the \mathbf{u} in VaDE is an emergent property of the model, whereas this Rademacher- \mathbf{u} is an imposed and potentially unnatural partitioning of the data.

This constructive method for defining a \mathbf{u} -task takes this method closer to the methods discussed in §2 and §5 based around learning a classifier on some defined \mathbf{u} -task – and much like in the

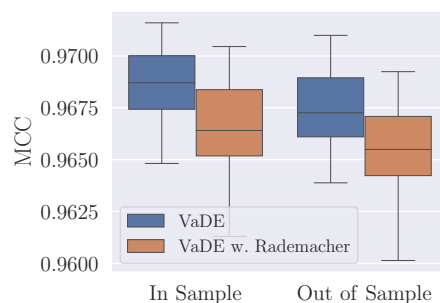


Figure C.2: MCC for Rademacher- \mathbf{u} and VaDE for $d_z = 50$, 128-component mixtures, MLP encoder and decoder, trained on CIFAR10.

contrastive-learning methods for self-supervised learning, here we are defining a \mathbf{u} variable from our data in an algorithmic way and then learning representations that connect to that choice of task. Recently JL methods have been used in non-Linear ICA, but in a different context: acting on the output of a flow to provide the means of a variational posterior (Camuto et al., 2021).

We are more interested in the naturally-emerging task of learning to cluster in \mathcal{Z} , as done in VaDE, but perhaps these more algorithmic approaches to obtain \mathbf{u} in an unsupervised setting could prove fruitful.

Appendix D. GMM-Flows

We also perform some experiments using flows (Papamakarios et al., 2019). We simply introduce a Gaussian Mixture Model $p_\theta(\mathbf{z}) = \sum_{\mathbf{u} \in \mathcal{U}} p_\theta(\mathbf{z}|\mathbf{u})p_\theta(\mathbf{u})$ as the flow’s base distribution and train under maximum likelihood,

$$\log p_\theta(\mathbf{x}) = \log p_\theta(\mathbf{z}) \left| \det \frac{\partial f_\theta^{-1}}{\partial \mathbf{x}} \right| \quad (\text{D.4})$$

where $\mathbf{x} = f_\theta(\mathbf{z})$ is the bijective mapping between \mathcal{Z} and \mathcal{X} .

We train an autoregressive flow of 10 layers on the same synthetic data as in the main paper, with batch size of 256, with a mixture model as the base distribution with 50 components. We find that these flows generally perform as well or better than iVAE or VaDE at discovering latent structure. Note that the iVAE and VaDE results are the same as in the main paper, Figure 2.

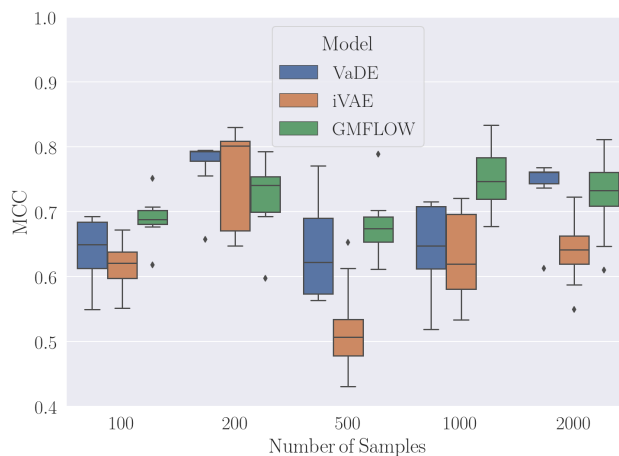


Figure D.3: MCC for VaDE, iVAE and GMM-Flow for synthetic data generated using $L = 4$ mixing.

Appendix E. Compute Resources

We used Azure Virtual Machines for the experiments on standard image datasets, NV series machines using M60 GPUs. As we said in the main paper, each individual run, training over image data, takes about 8h on average, though of course MLPs take less time, only a few hours, and ResNet runs take longer, about a day. Multiple runs can fit on a GPU at once.

The synthetic runs are much more lightweight – on a Dell XPS13 running Ubuntu these experiments run, over all datasets with their different numbers of datapoints, in about 6h for each VAE-derived model class, our GMM-flows taking about a day.